New Photorefractive Effect in Graded-Gap Superlattices

Stephen E. Ralph, Federico Capasso, and Roger J. Malik
AT&T Bell Laboratories, Murray Hill, New Jersey 07974
(Received 1 September 1989)

A photorefractive effect which results from the spatial separation of electrons and holes in compositionally graded semiconductors is demonstrated for the first time. Unlike conventional photorefractive effects, this nonlinear optical phenomenon requires only a single illumination beam, does not rely on the presence of traps, and is intrinsically very fast. The time evolution of the formation and decay of the space-charge electric field is measured via the electro-optic effect using picosecond pump and probe techniques.

PACS numbers: 78.65.−s, 73.50.Pz, 77.30.+d, 78.47.+p

Originally seen as undesirable optical damage, the photorefractive effect (PRE) is now the subject of intense research for image processing, optical phase conjugation, and associative memories.[1] The PRE is a nonlinear phenomenon which describes the optically induced change in the refractive index of a material. The conventional effect relies on the migration and trapping of nonuniformly photoexcited carriers resulting in an electro-optic effect via the induced space-charge field. The space charge is usually in the form of a grating created by the interference of two intersecting beams of coherent light. The grating is then used to diffract a third beam through an interaction length of several millimeters. The effect decays by the emission from traps and subsequent redistribution and recombination of charge carriers. Recently it has also been found that the nonequilibrium occupation of multiple defect states can lead to quenching of the PRE.[2]

In this Letter we report a new type of PRE which does not rely on traps, requires only a single illumination beam, and is inherently fast. The effect is efficient enough to cause significant phase retardation of the probe beam via the electro-optic effect, using only a short (2 μm) interaction length. Furthermore, the temporal response can be easily controlled by changing either the doping concentration or the photoinduced carrier density.

The graded-gap superlattice was grown by molecular-beam epitaxy (MBE) on ⟨001⟩-oriented semi-insulating undoped GaAs substrates. The structure was not intentionally doped and is residually p type $\sim 2\times 10^{15}$ cm^{-3}. Fifty periods of the graded-gap superlattice shown schematically in Fig. 1 were grown between two 2000-Å $Al_{0.7}Ga_{0.3}As$ window layers. The $Al_xGa_{1-x}As$ composition of each superlattice period was graded from $x=0.45$ to $x=0.35$ over 500 Å. The square quantum well (SQW) has a width of 40 Å which allows two confined electron subband levels. The second window layer was capped with a 100-Å GaAs layer. The high-quality analog compositional grading of the $Al_xGa_{1-x}As$ was achieved by growing the structure in an electron-gun source MBE machine.[3]

The graded alloy composition region and the narrow SQW provide two features necessary for an efficient photorefractive effect. In the graded-gap region the electrons and holes are spatially separated immediately after photoexcitation due to the large difference between the corresponding velocities. The latter arises from the large difference between the quasielectric fields acting on the electrons and holes[4] and the different effective masses. The SQW enhances the photorefractive effect by acting as a large trap, which allows the photoexcited electrons to accumulate in a thin region and thereby maximizes the space-charge separation.

The photoexcited electrons move to the SQW in a

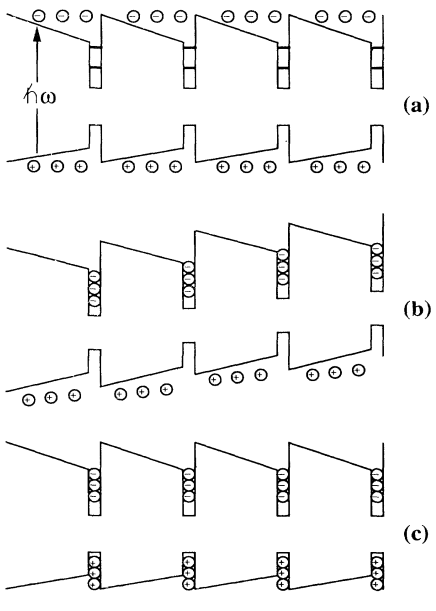

FIG. 1. Schematic energy-band diagram of the compositionally graded superlattice: (a) during photoexcitation; (b) immediately after photoexcitation, the electrons have moved to the SQW under the influence of the conduction-band quasifield; (c) at a later time, the holes have moved to the SQW eliminating the space-charge field.

time ≤ 0.5 psec estimated by taking an electron velocity of $\geq 10^7$ cm/sec in the conduction-band quasielectric field of ≈ 18 kV/cm.[5] The latter results from the sum of the quasifield due to the grading (15 kV/cm) and the space-charge field (~ 3 kV/cm) arising from the accumulation of holes in the SQW, generated by charge transfer from the acceptors in the graded region.[6] On the other hand, holes experience a quasielectric field $F \approx 5$ kV/cm equal to the difference between the field due to the grading (8 kV/cm) and the above space-charge field. The hole velocity can then be estimated from $\mu_{hh}F$ to be $\approx 2\times 10^5$ cm/sec, taking $\mu_{hh} \approx 40$ cm^2/V sec.[7] These estimates show that the space-charge field in our structures is set up in a subpicosecond time. This is much faster than the rise times commonly found in photorefractive materials which rely on multiple trapping and emission to establish the space-charge field. As we shall see the separation of carriers depicted in Fig. 1(b) creates, in our experiments, fields of a few kV/cm.

The subsequent decay of the space-charge field is an extremely nonlinear process. The complexity of the decay process is partly due to nonuniform absorption which creates a concentration gradient of holes, decreasing with increasing band gap. The space-charge field decays by hole drift and diffusion. Holes move toward the SQW under the influence of the combined effects of the quasifield, the photoinduced space-charge field, and the concentration gradients. The latter will act in a direction opposing that of the other fields. Taking these effects into account leads to an estimate for the time required by the holes to transfer into the SQW of ≈ 40–70 psec.

We can model the profile of the photogenerated holes from the absorption coefficient[8] which is proportional to $(\hbar\omega - E_g)^{1/2}$. The carriers generated in the SQW do not contribute to the space-charge field since they are not spatially separated and are therefore not included in the estimate of the photovoltage. Using the absorption coefficient to calculate the carrier distribution immediately after pumping, and assuming all the electrons have moved to the SQW, the peak photoinduced voltage across the structure is well approximated by

$$V = \frac{3}{5}\frac{Nd^2\bar{\rho}}{\epsilon}, \tag{1}$$

where d is the length of a single graded region, N is the number of superlattice periods, and $\bar{\rho}$ is the photogenerated hole density averaged over all the graded regions.

For the experiments large (0.5 and 1.0 mm) openings were etched through the substrate to eliminate absorption effects in the substrate. A selective etch was used in the final step to stop uniformly at the back $Al_xGa_{1-x}As$ window. The remaining membrane was only 3 μm thick and was left free standing.

The pump-probe experimental setup consisted of a 100-MHz harmonically mode-locked yttrium aluminum garnet laser which produced 50-psec pulses with 10 W of average power. The 1.06-μm light was split 75:25 with the 75% portion frequency doubled in a $LiIO_3$ crystal. The second harmonic was used to synchronously pump a dye laser. The dye laser produced a 4-psec pulse with 150 mW of average power and was used to create the free carriers. The remaining 25% of the 1.06-μm beam was pulse compressed in a fiber-grating pulse compressor. This synchronous 1.06-μm pulse was 2 psec long and was used to probe the induced birefringence. The probe beam was focused to a diameter of 50 μm which was intentionally smaller than the pump beam which was focused to a 75-μm diameter. The larger pump focus allows the probe beam to sample a more uniformly pumped region. The pump beam is chopped with an acousto-optic modulator at 31 kHz and the 1.06-μm probe beam is synchronously detected using standard lock-in techniques. The structure is transparent to the probe beam.

The electric field created by the separation of electrons and holes produces a birefringence which, in crystals with $\bar{4}3m$ symmetry, can be described by an index ellipsoid with principal axes aligned along the $\langle 110\rangle$ directions [X' and Y' in Fig. 2(a)].[9] If a linearly polarized beam is oriented along a principal axis, the transmitted intensity is insensitive to the birefringence since only the phase has changed. However, if the linearly polarized beam is oriented at some angle with respect to the two principal axes, its components along the principal axes experience unequal phase shifts. This produces a polarization rotation of the transmitted beam. For circularly polarized (CP) light the birefringence causes the circularly polarized beam to become elliptically polarized. The differential phase shift, called retardation, can then be accurately measured by differentially detecting appropriate orthogonal polarizations (separated by a polarizing beam splitter) of the transmitted probe beam. The phase retardation between the Y' and X' polarizations of circularly polarized light, after propagating through the crystal, is given by[9]

$$\Gamma = \frac{2\pi}{\lambda}n^3 r_{14} V + \frac{\pi}{2}, \tag{2}$$

where n is the refractive index, r_{14} is the electric-optic coefficient, and V is the voltage across the crystal. If the relative angle between one of the index ellipse principal axes (e.g., X') and one of the axes of an analyzer, which establishes the two observed polarization directions, is ϕ as in Fig. 2, then the ratio of the transmitted intensity (I_{tX}) with polarization along X to the total incident intensity (I_i) is given by

$$\frac{I_{tX}}{I_i} = \tfrac{1}{2}\{1 - \sin(2\phi)\cos(\Gamma)\}. \tag{3}$$

It is clear from (3) that for a constant retardation Γ, the intensity of the transmitted polarization is cyclical in ϕ. Thus, by rotating the sample 360° about an axis perpendicular to the $\langle 001\rangle$ surface, the signal level will oscillate

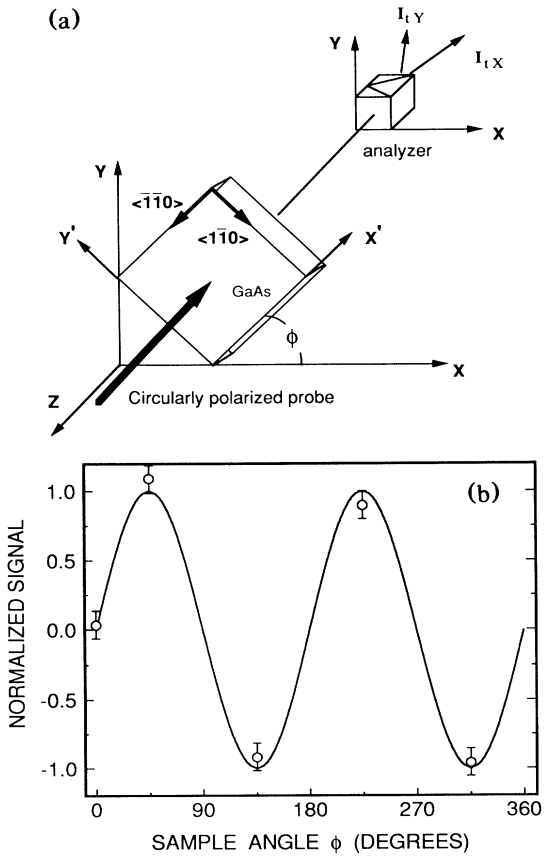

FIG. 2. Schematic of the electro-optic measurement technique used to measure the photoinduced space-charge field. The probe beam is circularly polarized before entering the graded-gap structure. The induced birefringence is observed as a difference signal between the two orthogonal polarizations X and Y. Inset: The peak value of the measured signal $[(I_{tX}-I_{tY})/I_{iX}]$ (normalized to unity) as a function of sample angle together with the expected angular dependence (continuous line) given by Eq. (4). The angle refers to the relative inclination of the crystal ⟨011⟩ direction with respect to the X axis of the analyzer.

through two periods with maximum signal levels occurring when the ⟨110⟩ crystal axes are 45° with respect to the detected polarization directions.

There is an expression similar to (3) for the transmitted Y polarization. By subtracting the two detected signals (X-Y) the dc component of the signal (and the associated noise) is removed and the signal strength doubles. The difference signal, now normalized to a single polarization component ($I_{iX}=I_{iY}$), is given by

$$\frac{I_{tX}-I_{tY}}{I_{iX}}=2\sin(2\phi)\sin(\Gamma_0)\approx 2\sin(2\phi)\Gamma_0\,, \qquad (4)$$

where Γ_0 is just the field-dependent part of Γ in (2) and $\sin(\Gamma_0)$ has been approximated by the argument since typically $\Gamma_0 \leq 10^{-4}$ rad.

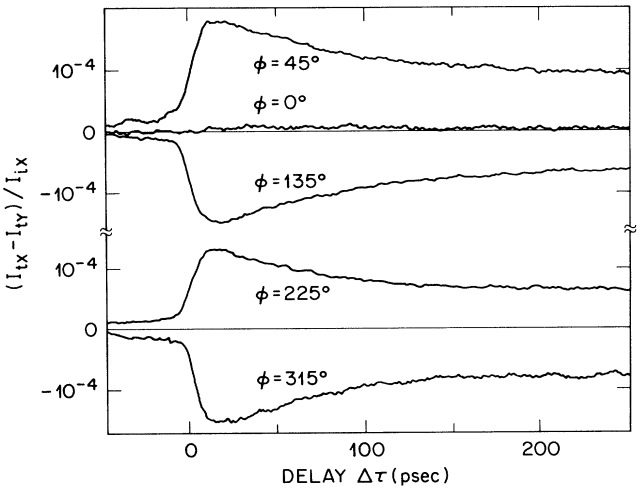

FIG. 3. The measured electro-optic effect as a function of delay between the pump and probe pulses. The data for the five different sample positions of Fig. 2 are shown. The signal depicted is the difference between two transmitted orthogonal polarizations of the initially circularly polarized probe beam normalized to the intensity of a single polarization. Note that for the angles 45°, 135°, 225°, and 315°, the magnitude of the signal is equal to the retardation $2\Gamma_0$ [see Eq. (4)].

The peak value of the measured signal $[(I_{tX}-I_{tY})/I_{iX}]$ is shown in Fig. 2(b) as a function of sample angle ϕ. The response clearly follows (4) with the zeros and maxima occurring at the proper orientations. This is an unambiguous signature of the electro-optic effect and, therefore, of a macroscopic electric field. Figure 3 shows the measured signal as a function of delay for five different sample orientations. The rise time of the signal is limited by the pulse-to-pulse jitter which was measured by two-photon absorption in GaP to be 10 psec. The decay of the signal is exponential in the first 100 psec after the pump pulse with a time constant of 80 psec. Holes which move unhindered toward the SQW are responsible for this decay time; the measured time constant compares favorably with the previously estimated hole transit time. The initial fast decay is followed by a slowly decaying tail with a time constant of 1–2 nsec. This longer time constant is likely due to trapping and release of holes by ionized acceptor states in the AlGaAs. Deep donors associated with the DX or $EL2$ center may also contribute to the long decay, by becoming ionized during illumination. The excellent symmetry of the data also confirms the absence of any absorption affects. It is important to note that recombination, which occurs in the SQW, does not affect the time evolution of the signal since it does not change the distance between the centroids of the hole and electron charge distributions.

Using $\lambda=1.06$ μm, $n=3.48$, $r_{14}=1.4\times10^{-14}$ cm/V, and Eq. (2), the total voltage across the sample is given

by $(\Gamma_0/3.0\times10^{-4})$ V. For the data of Fig. 3, the peak photovoltage is 0.25 V. This corresponds to an average space-charge field strength of 1 kV/cm. The estimate of the expected induced voltage and field strength requires a careful assessment of the power absorbed in the graded-gap region. From the absorption measurements and calculations one can show that nearly half of the pump power is absorbed in the SQW. This corresponds to an absorption coefficient of 2.8×10^4 cm^{-1} at the pump wavelength.[10] From the experimental parameters of 6-mW average pump power at 6100 Å ($\alpha=1000$ cm^{-1}, in the graded region) the expected average carrier density in the graded-gap region is $\bar{\rho}=4.6\times10^{15}$ cm^{-3}. Using Eq. (1), a total voltage of 0.48 V is expected across the entire structure. Thus our measured retardation corresponds to a photoinduced voltage which is of the order of the value estimated from the photogenerated carrier density. The time response may be controlled through the photoexcited carrier density which determines the induced space-charge field. The response did become faster with increasing pump power as expected.

Note that time-varying space-charge fields associated with the macroscopic polarization of asymmetric quantum wells gives rise to a displacement current which can be detected via photocurrent experiments.[11]

The induced birefringence was measured for a variety of pump wavelengths. For a pump energy of 1.92 eV most of the created carriers were near the minimum of the graded structure with the majority of carriers created in the SQW and a small electro-optic effect was measured. The highest pump energy, 2.07 eV, created carriers throughout the entire graded structure and produced a large electro-optic effect. The decrease in signal is anticipated since the number of photoexcited electron-hole pairs and the separation of the centroids of the holes and electrons both decrease with increasing wavelength.

As a further test of the importance of the graded-gap structure, a reference sample with the superlattice replaced by a GaAs region was grown and processed identically to the sawtooth superlattice structure. This reference structure did not show any electro-optic effect.

Finally, it is interesting to compare this effect with the conventional PRE. The graded-gap structures reported here have an intensity modulation of 1×10^{-4} with a 2-pJ/μm^2 fluence. Short creation times for conventional photorefractive effects in GaAs have been reported with efficient intensity modulation; however, the effect requires pump fluences of 0.3 mJ and has an unreported decay time.[12]

[1]A. M. Glass and J. Strait, in *Photorefractive Materials and Their Applications,* edited by P. Gunter and J. P. Huignard (Springer-Verlag, New York, 1988); J. Feinberg, Phys. Today **41**, No. 10, 46 (1988); J. P. Huignard, J. P. Herriau, P. Aubourg, and E. Spitz, Opt. Lett. **4**, 21 (1979); D. Z. Anderson, Mater. Res. Bull. **13**, 30 (1988).

[2]D. D. Nolte, D. H. Olson, and A. M. Glass, Phys. Rev. Lett. **63**, 891 (1989).

[3]R. J. Malik, J. Vac. Sci. Technol. B **5**, 722 (1987).

[4]H. Kroemer, RCA Rev. **18**, 332 (1957).

[5]B. F. Levine, C. G. Bethea, W. T. Tsang, F. Capasso, K. K. Thornber, and R. C. Fulton, Appl. Phys. Lett. **42**, 769 (1983).

[6]J. A. Hutchby, J. Appl. Phys. **49**, 4041 (1978).

[7]S. Tiwari, J. Hintzman, and A. Callegari, Appl. Phy. Lett. **51**, 2118 (1987).

[8]J. I. Pankove, *Optical Processes in Semiconductors* (Prentice Hall, Englewood Cliffs, NJ, 1971).

[9]A. Yariv, *Quantum Electronics* (Wiley, New York, 1967).

[10]H.-C. Lee, A. Kost, M. Kawase, A. Hariz, P. D. Dapkus, and E. Garmire, IEEE J. Quantum Electron. **24**, 1581 (1988).

[11]F. Capasso, S. Luryi, W. T. Tsang, B. Levine, and C. G. Bethea, Phys. Rev. Lett. **51**, 2318 (1983).

[12]A. L. Smirl, G. C. Valley, R. A. Mullen, K. Bohnert, and T. F. Boggess, Opt. Lett. **12**, 501 (1987).